



# DIVALENT METAL IONS DOPED NiFe<sub>2</sub>O<sub>4</sub> FOR MAGNETIC AND GAS SENSING STUDIES

Shilpa S<sup>1</sup>, Chivukula Srikanth<sup>2</sup>, Hemalatha K S<sup>3</sup>, Syeda Ayesha<sup>4</sup>, S. Abdul Khader<sup>5\*</sup>, Asiya Parveez<sup>5</sup>

<sup>1</sup> Department of Physics, Govt. First Grade College, Kadugudi, Bengaluru-560067, Karnataka, India.

<sup>2</sup>Department of Physics, Govt. College (Autonomous), Kalaburagi -585105, Karnataka, India.

<sup>3</sup>Department of Physics, Maharani's Science College for Women, MCU, Bangalore-560001.

<sup>4</sup>Department of Chemistry, Govt. First Grade College, Kuvempunagar-570023. Mysore, Karnataka.

<sup>5</sup>Department of Physics, Govt. Science College, Chitradurga-577501, Karnataka, India.

**Corresponding Author:** S Abdul Khader, [khadersku@gmail.com](mailto:khadersku@gmail.com)

## Abstract:

Magnetic and gas sensing studies of divalent metal ions doped nickel ferrite, divalent metal ions such as Mg<sup>+2</sup>, Cu<sup>+2</sup> and Co<sup>+2</sup> were substituted in pure Nickel ferrite (NiFe<sub>2</sub>O<sub>4</sub>) with the basic composition Ni<sub>0.5</sub>M<sub>0.5</sub>Fe<sub>2</sub>O<sub>4</sub> (here, M= Mg<sup>+2</sup>, Cu<sup>+2</sup> and Co<sup>+2</sup>), which were synthesized by auto-combustion method using, nitrate-citrate method. As-prepared samples were sintered at 950°C and investigated for various properties. Single phase spinel cubic structure was confirmed for the proposed samples by X-ray diffraction (XRD) studies. Surface morphology of the samples were probed using FESEM. For the proposed nano-powder samples magnetic measurements were done at RT using Vibrating Sample Magnetometer (VSM). Gas sensing measurements were done at room temperature for the synthesized samples to check their sensitivity towards NO<sub>2</sub> gas.

**Keywords:** Impedance; Dielectric; Nano-powders; Magnetic; Auto-combustion.

**DOI Number:** 10.14704/nq.2021.19.9.NQ21154

**NeuroQuantology 2021; 19(9): 804-810**

## Introduction

Mostly used ferrites in the ferrite family are spinel ferrites. Nano structured soft spinel ferrites have attracted great interest due to their excellent physio-chemical properties such as, low toxicity and their magnetism as well as, because of their highly tunable properties, like its dielectric, magnetic properties, which can be easily modified just adopting various preparation techniques and various factors such as the type of organic fuel used for the synthesis, P<sub>H</sub> of the redox solution, composition of the metal ions, crystal structure, types of additives and sintering temperature etc [1-3]. These nano-structured magnetic oxides are currently considered among the widely successful magnetic nanoparticles (MNPs) that can be extensively used for various technological and in medical applications such as electrochemical sensor applications, in storage medium, contrast enhancement in magnetic resonance imaging,

suspension systems using magnetic fluids, targeted drug delivery and in many more technological devices and applications. [4-5]. Spinel magnetic oxide materials, mainly consists of Fe<sub>2</sub>O<sub>3</sub> and have spinel (MFe<sub>2</sub>O<sub>4</sub>) cubic structure, here M is a divalent metal ion such as Co<sup>+2</sup>, Zn<sup>+2</sup>, Mg<sup>+2</sup>, Ni<sup>+2</sup>, Cd<sup>+2</sup>, Cu<sup>+2</sup> or a combination of these ions. These samples, which are ferri-magnetic in nature exhibit magnetic hysteresis (M-H curve) and at the same time exhibit spontaneous magnetization. Various properties of magnetic spinel is because of distribution of divalent and trivalent metal ions among the available voids such as tetrahedral (A) and octahedral (B) sites [5]. For any materials of interest, its properties are highly dependent on preparation technique adopted, type of synthesis environment such as in inert or in open air atmosphere, type of organic fuel used, sintering time and temperature, etc.



In case of inverse spinel structure half of the trivalent metal ions occupy tetrahedral (A-sites) and half in octahedral (B-sites), the remaining cations being randomly distributed among the B-sites. Inverse spinel ferrites are represented by the formula (Me<sup>+3</sup>)<sub>A</sub> [M<sup>+2</sup>Me<sup>+3</sup>]<sub>B</sub>O<sub>4</sub>. Nickel ferrite belongs to inverse spinel with Ni<sup>+2</sup> at octahedral (B-site) and Fe<sup>+3</sup> ions distributed equally in both, tetrahedral (A-site) and octahedral sites (B-site). Nickel ferrites are used in numerous electronic device applications because of their high permeability, high electrical resistivity, mechanical hardness, and chemical stability [6-10].

Samples of divalent metal ions substituted nickel ferrite are the technologically important materials which are used in functional devices such as in field sensors, heterogeneous catalysis, and in various sensors [11].

In our present study, samples of divalent metal ions substituted nickel ferrite with the basic composition Ni<sub>0.5</sub>M<sub>0.5</sub>Fe<sub>2</sub>O<sub>4</sub> (here M= Mg<sup>+2</sup>, Cu<sup>+2</sup> and Co<sup>+2</sup>) were prepared using nitrate-citrate auto-combustion method. This method is a self-propagating thermally-induced reaction of a gel, obtained from aqueous solutions containing metallic nitrates which acts as oxidizer and an organic fuel. Stoichiometric proportions between fuel and metallic nitrates are calculated according to the valencies of the reacting elements so as to provide the relation of oxidizer/fuel equal to one [12]. Here, metallic nitrates are preferred as starting materials which are also known as precursors, because of their water-soluble nature, have low ignition temperatures and are easy to prepare.

### Materials and methods

Nano-powders of divalent metal ions substituted NiFe<sub>2</sub>O<sub>4</sub> ferrite samples of Ni<sub>0.5</sub>M<sub>0.5</sub>Fe<sub>2</sub>O<sub>4</sub> a, here M = Mg<sup>+2</sup>, Cu<sup>+2</sup> and Co<sup>+2</sup> were prepared using auto-combustion method. Precursors for starting the materials synthesis are Nickel Nitrate (Ni (NO<sub>3</sub>)<sub>2</sub>.6H<sub>2</sub>O), Ferric Nitrate (Fe (NO<sub>3</sub>)<sub>2</sub>.9H<sub>2</sub>O), Magnesium Nitrate (Mg (NO<sub>3</sub>)<sub>2</sub>.6H<sub>2</sub>O), Copper Nitrate (Cu (NO<sub>3</sub>)<sub>2</sub>.3H<sub>2</sub>O), Cobalt Nitrate (Co (NO<sub>3</sub>)<sub>2</sub>.6H<sub>2</sub>O) and Citric acid (C<sub>6</sub>H<sub>8</sub>O<sub>7</sub>.H<sub>2</sub>O), all chemicals are of AR Grade with purity more than 99%.

Aqueous solutions of metallic nitrates and Citric acid, which is here taken as organic fuel needed for auto-combustion reaction and are taken as per the stoichiometry. Equi-molar citric acid was added into the aqueous solution of metallic nitrates. Aqueous solution containing redox mixture was taken in a silica crucible and is allowed in to a muffle furnace, which was already pre-heated to a temperature of 550°C. Redox mixture finally yields porous and fluffy voluminous ferrite powder. Obtained fluffy material was ground to get ferrite powders. As-burnt ash was sintered at 950°C for 4 hours to get better crystallization and homogeneous cation distribution in the proposed spinel and finally ground to get proposed ferrite nano-powders. Phase confirmation of the proposed samples were investigated using X-ray diffraction (XRD) studies using Bruker AXS D8 Advance X-ray diffractometer (using Cu-K<sub>α</sub> radiation, λ=1.5406 Å), a working voltage of 40kV at 40mA of current. Diffraction data were collected in the 2θ range 10-80°. Morphology of the sintered samples has been investigated using Field Emission Scanning Electron Microscope (JEOL Model 7610FPLUS). Magnetic measurements were performed using vibrating sample magnetometer VSM, Lakeshore Model: 7400, USA.

805

### Results and discussion

#### Phase and Surface Morphology

XRD patterns of the proposed samples of the system Ni<sub>0.5</sub>M<sub>0.5</sub>Fe<sub>2</sub>O<sub>4</sub> (here M= Mg<sup>+2</sup>, Cu<sup>+2</sup>, Co<sup>+2</sup>) are presented in Figure 2(a) and Fig 2 (b). Presence of (220), (311), (400), (422), (511), (440) and (533) planes indexed for the cubic phase of spinel ferrites [ For Ni<sub>0.5</sub>Mg<sub>0.5</sub>Fe<sub>2</sub>O<sub>4</sub>, JCPDS Card No: 52-0278 and JCPDS Card No: 77-0010 for Ni<sub>0.5</sub>Cu<sub>0.5</sub>Fe<sub>2</sub>O<sub>4</sub> and for Ni<sub>0.5</sub>Co<sub>0.5</sub>Fe<sub>2</sub>O<sub>4</sub>, JCPDS Card No: 25-0283]. Synthesized nano-samples were labelled as NMg-2 (Ni<sub>0.5</sub>Mg<sub>0.5</sub>Fe<sub>2</sub>O<sub>4</sub>), NCu-2 (Ni<sub>0.5</sub>Cu<sub>0.5</sub>Fe<sub>2</sub>O<sub>4</sub>) and NCo-2 for Ni<sub>0.5</sub>Co<sub>0.5</sub>Fe<sub>2</sub>O<sub>4</sub>. Microstructures were studied by placing the samples under Scanning electron microscope. Micrographs of the sintered samples are depicted in Fig. 1 (a-c), shows the surface structure for the proposed samples. All the

samples are having well dispersed, dense and well defined granular structure.

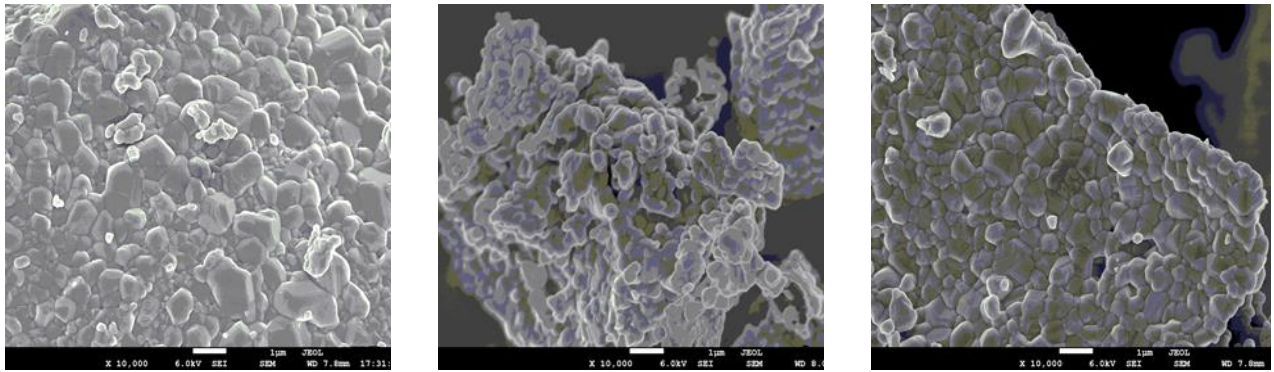


Fig. 1 Micrographs of (a) Ni<sub>0.5</sub>Mg<sub>0.5</sub>Fe<sub>2</sub>O<sub>4</sub> (b) Ni<sub>0.5</sub>Cu<sub>0.5</sub>Fe<sub>2</sub>O<sub>4</sub> (c) Ni<sub>0.5</sub>Co<sub>0.5</sub>Fe<sub>2</sub>O<sub>4</sub>

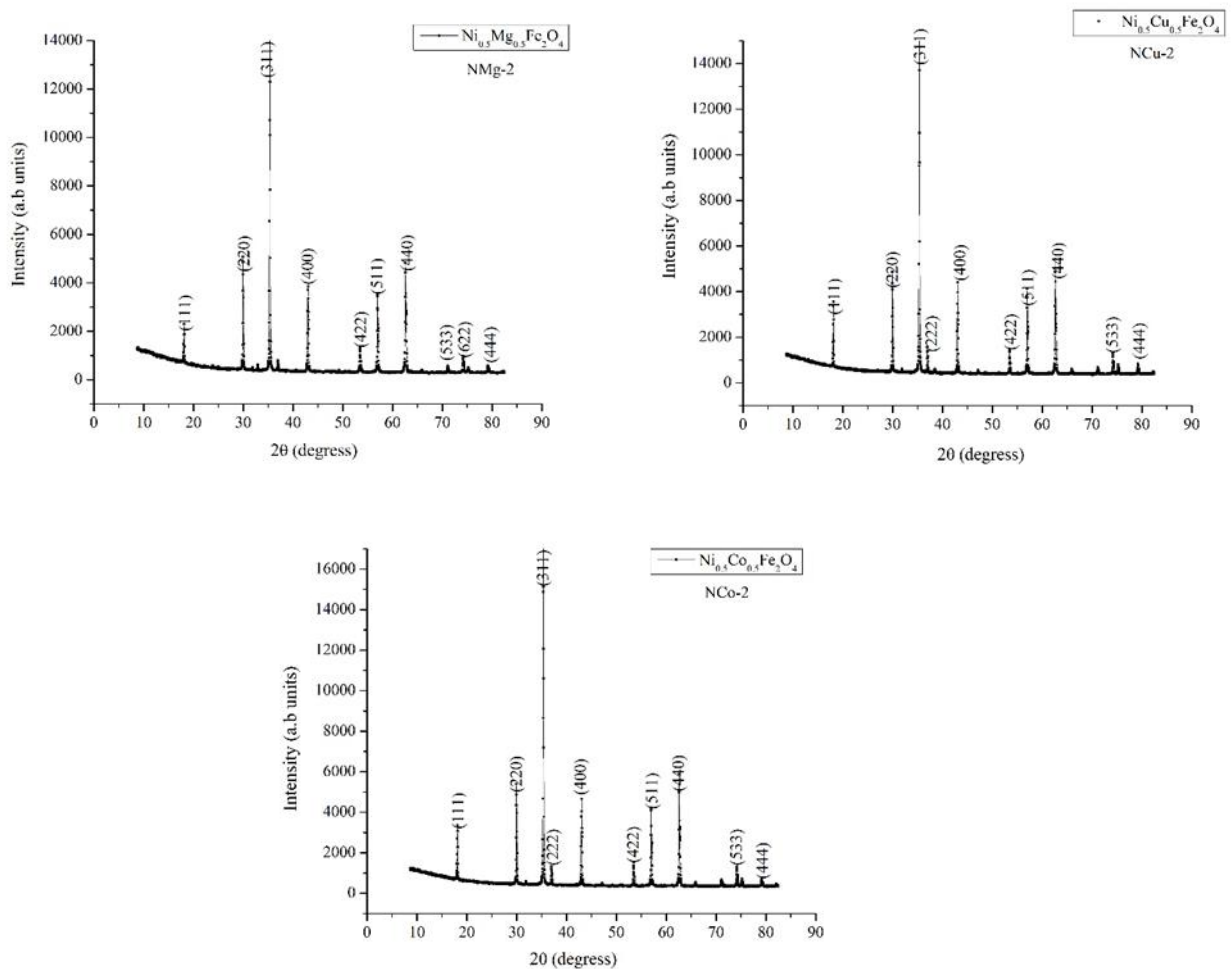


Fig. 2. XRD Spectrum of (a) Ni<sub>0.5</sub>Mg<sub>0.5</sub>Fe<sub>2</sub>O<sub>4</sub>, (b) Ni<sub>0.5</sub>Cu<sub>0.5</sub>Fe<sub>2</sub>O<sub>4</sub> and (c) Ni<sub>0.5</sub>Co<sub>0.5</sub>Fe<sub>2</sub>O<sub>4</sub>

### Magnetic Studies

M-H loops, at RT were recorded for all the divalent metal ions substituted samples and are shown in Fig.3.1. From, M-H loops, it is clear that loops are saturated at higher field values, which is the characteristic feature of

any ferromagnetic material. Proposed samples exhibited no hysteresis, which may be attributed to super paramagnetic nature of the samples. Magnetic parameters such as M<sub>s</sub>, M<sub>r</sub>, H<sub>c</sub>, SR and K were extracted from the obtained M-H loops [13-19]. Magnetic anisotropic

constant (K) can be related to M<sub>s</sub> and H<sub>c</sub> given by  $K = M_s H_c / 0.96$ . Squareness ratio (SR) measures, how square is the hysteresis loop. For applications like memory devices, SR should be as large as possible but for magnetic fluids, it should be as low as possible. Magnetic anisotropic constant, K originating from the presence of Fe<sup>+2</sup> ions in the ferrites is the key parameter for understanding and for tuning the superparamagnetic properties of the nanoparticles (NPs) and this anisotropic constant is a function of both temperature and particle size of the synthesized NPs. According to Stoner –Wohlfarth, the magnetic anisotropy E<sub>A</sub> of a single domain particle can be expressed as:

$E_A = KV \sin^2 \theta$ , here V is the volume of the nanoparticle,  $\theta$  is the angle between the magnetization direction and the easy axis of the nanoparticle. This anisotropy serves as the energy barrier to prevent the change of magnetization direction [20]. Magnetic anisotropic constant, K, can be calculated by the law of approach method [21], given by  $K = M_s H \{13.125 (1 - M/M_s)\}^{0.5}$ . Here M<sub>s</sub>, H, M represents saturation magnetization, applied magnetic field and magnetization. Measured magnetic parameters for all the samples under the applied magnetic field (H) are summarized in Table 1.

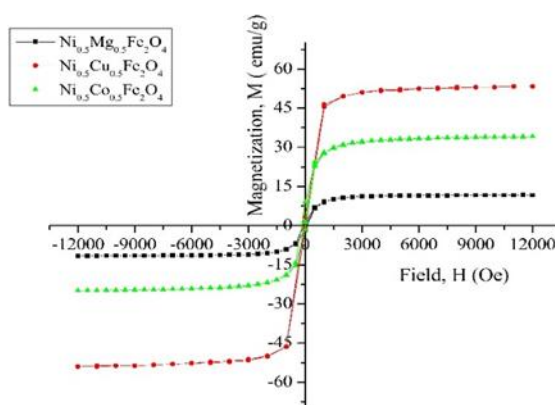


Fig. 3.1. Magnetic Hysteresis loops of Ni (Mg, Cu, Co) Fe<sub>2</sub>O<sub>4</sub> Nano-powders.

Table 1. Magnetic parameters obtained from M-H Loops.

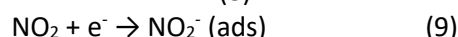
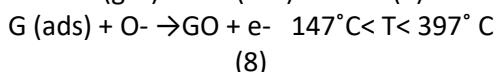
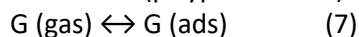
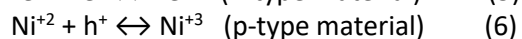
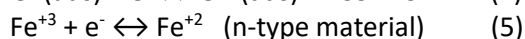
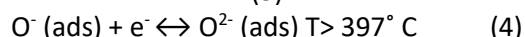
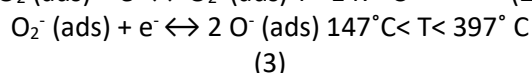
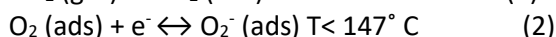
Sample(s)	Saturation Magnetization <b>M<sub>s</sub></b> (emu/g)	Remanent Magnetization <b>M<sub>r</sub></b> (emu/g)	Coercive Field <b>H<sub>c</sub></b> (Oe)	Anisotropic Constant, <b>K</b> (erg/Oe)	Squareness ratio ( <b>SR</b> )
Ni <sub>0.5</sub> Mg <sub>0.5</sub> Fe <sub>2</sub> O <sub>4</sub>	11.72	1.3	105.25	1286	0.11
Ni <sub>0.5</sub> Cu <sub>0.5</sub> Fe <sub>2</sub> O <sub>4</sub>	53.88	3.39	19.52	1085	0.06
Ni <sub>0.5</sub> Co <sub>0.5</sub> Fe <sub>2</sub> O <sub>4</sub>	34.41	9.004	33.78	1210	0.26

### Gas Sensing Studies

In this, the potentiality of the spinel structure ferrites doped with divalent metal ions is explored for gas sensing particularly for NO<sub>2</sub> gas (for 100ppm). Change of resistance usually mentioned as R<sub>a</sub>/R<sub>g</sub>, where R<sub>a</sub>, the resistance in air, R<sub>g</sub>, the resistance of the sensor after exposing to the gas, is the response which is the main performance of a gas sensor [21-22].

When doped ferrite samples based sensor is exposed to the air, the oxygen molecules in the air will chemisorb onto the metal oxide particle, capturing the electrons and transforms into O<sub>2</sub><sup>-</sup>, O<sup>-</sup> or O<sub>2</sub><sup>-</sup> which specifically depends on temperature shown in equations (1) to (4). Mechanism of NO<sub>2</sub> detection of tested sensors (samples) at RT can be

explained by the chemisorption and removal of the surface chemisorbed species.



Electron transfers that occur in equations (2) – (4) cause the formation of the depletion layer on the materials surface, making the conductive channel narrow with the increase of R<sub>a</sub> (Resistance in air). During the sensing process, the chemisorbed oxide particle can capture electrons, changing Fe<sup>+2</sup> to Fe<sup>+3</sup>, which is shown in equation (5). In p-type material, the hole becomes the carrier as per equation (6). On account of the dissociation effect of oxygen, the valency distribution and defects in the crystal structure changed, while a part of the conductive three-dimensional network

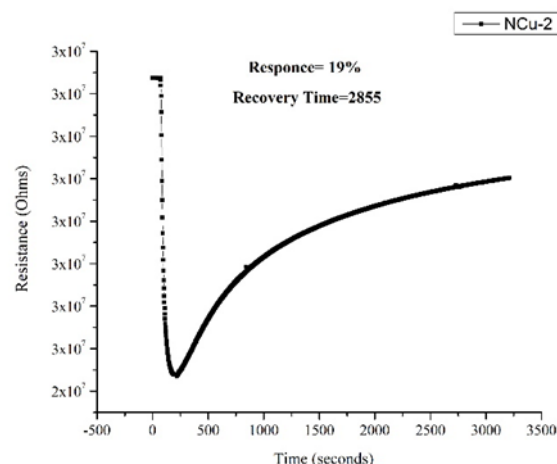
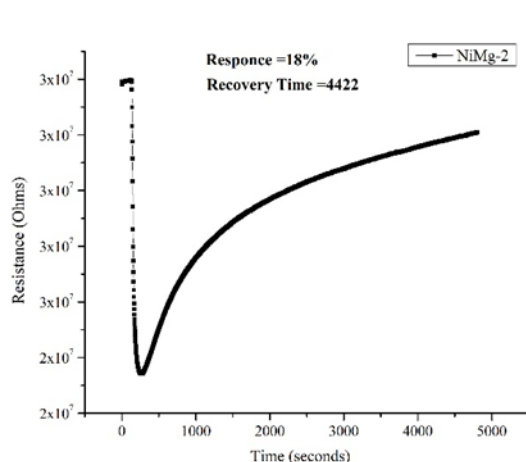
structure is cut off, so that the R<sub>a</sub> of the material increases [21-22].

When the reduced gas diffuses to the surface of the sensitive material, it will rapidly undergo a redox reaction, with the oxygen on the surface. During the reaction, electron captured by oxygen will return to the material, and the resistance will be altered means decreases. According to the sensing mechanism, the possible reacting processes to reduced gas are as per the equations (7) and (8). Detailed reaction will change with the operating temperature. Similar explanation follows for the remaining series of composite samples. Sensing response of doped NiFe<sub>2</sub>O<sub>4</sub>, samples are mentioned from Fig.3.2.

Obtained sensing parameters for NO<sub>2</sub> gas sensing is tabulated in Table.2. From the obtained data, it is clear that among the doped samples Ni<sub>0.5</sub>Cu<sub>0.5</sub>Fe<sub>2</sub>O<sub>4</sub>- NCu-2 shown good sensing properties in when compared to remaining two samples in terms of response time and recovery time, it is because of the surface properties of the sample such as its particle size, porous structure of the sample, which can be further confirmed from optical microscopy studies (FESEM) [23-25].

Table 2. Gas sensing parameters obtained from sensing measurements.

Sample	Response of sensor in percentage	Recovery time in seconds
NiMg-2	18	4422
NCu-2	19	2855
NiCo-2	14	1570



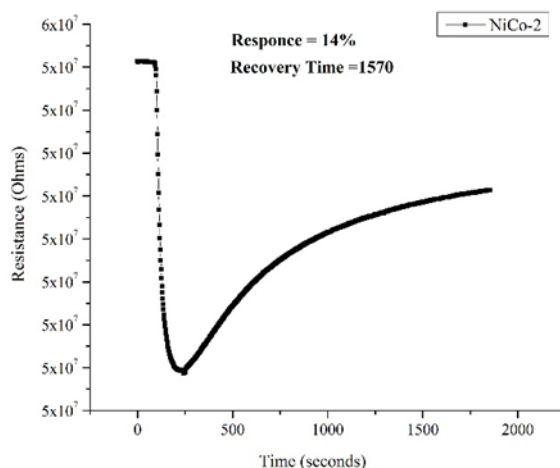


Fig.4. Sensing response of Ni (Mg, Cu, Co) Fe<sub>2</sub>O<sub>4</sub> nano-powders.

### Conclusions

Nano-powders of the system Ni<sub>0.5</sub>M<sub>0.5</sub>Fe<sub>2</sub>O<sub>4</sub> (here M=Mg<sup>2+</sup>, Cu<sup>2+</sup>, Co<sup>2+</sup>) were prepared successfully using auto-combustion method which involves nitrate-citrate precursors. Structural phase is confirmed through PXRD studies for the divalent metal ions doped NiFe<sub>2</sub>O<sub>4</sub> nano samples.

Morphology of the nano-powders reveals the dense structures with well-defined grains. From magnetic studies, it is observed that, the proposed samples with narrow hysteresis loop were synthesized with low values of coercivity. Hence, these samples are magnetically soft materials. All the proposed samples responded to NO<sub>2</sub> gas, enabling them suitable candidates for NO<sub>2</sub> detection or sensing.

Finally, it is concluded that, series of divalent metal ions doped ferrite samples have been studied for magnetic and gas sensing properties. These characteristics of the proposed nano-powder samples are of technologically important and can be implemented in multi-functional device applications.

### Acknowledgements

Authors are highly thankful to CENSE, IISc-Bangalore for providing PXRD and FESEM facilities to accomplish this research work.

### References

1. Fish G. E Soft magnetic materials, Proc.IEEE,78, pp.947-972 (1990).

2. Prathapani S, Vinitha M, Jayaraman T V, Das D, Jour. Appl.Phys, 115, p.17A502 (2014).
3. Alqarni A. N, Almessiere M A, Guner S, Sertkol M, Tashkandi N, Shirsath S E, Baykal A, Ceramic.Int, 48, pp.5450-5458 (2022).
4. Valenzuela R, Phys. Res.Int, 2012 (2012).
5. Pillai V, Shah D. O, Jour. Magn.Magn. Mater, 163, pp.243 (1996).
6. Mohamed M.B, Appl. Phys. A: Mater. Sci. Process, 125, pp.1-10 (2019).
7. Kumar R, Kumar H, Singh R R, Barman P.B, AIP.Conf. Proc, 1675, 030003 (2015).
8. M.Lakshmi, K.Vijaya kr, K.Thyagarajan, J.Nano.struct in Chem, 5(4), pp.365 (2015).
9. Abdallah H M I, Moyo T, Ngema N, Jour.Magn.Magn. Matr, 394, pp.223-228 (2015).
10. A.B Bodade, H.G Wankhade, G.N Chaudhari, D.C Kothari, Talanta, 89, pp.183 (2012).
11. S.Abdul Khader, Asiya Parveez, Arka Chaudhuri, M S Shekhawat and T.Sankarappa, Physica B: Condensed Matter, 584, May Issue, pp.411675 (2020).
12. K. Mukherjee, S.B Majumder, Jour. Talanta, 81, pp.1826-1832 (2010).
13. S.Andris, G.A Karlis, Sens. Actuators B, 222, pp.95-105 (2016).
14. Wagner KW (1913) Ann Phys 40:817.
15. Maxwell JC, Electricity & Magnetism, Vol 1, Oxford Univ Press, Oxford (1929).
16. Koops CG (1951) Phys Rev 83:121.
17. J.Smitet H.P, J Wijn, Les.Ferrites, Dunod, Paris (1961).

18. P. Singh, D. Rathore, Jour. Appl. Phys, 1728, pp.20259 (2016).
19. Chikazumi S, Physics of Ferromagnetism, Oxford University Press, Oxford (1997).
20. E.C Stoner and E.P Wohlfarth. Phil. Trans. Roy. Soc.A 240, 599 (1948).
21. P. Shankar and J.B. B Rayappan, Sci.Lett. J, 4, pp.126 (2015).
22. G. Eranna, Solid state Gas Sensing, Springer Publications (2009).
23. D. Rathore, R. Kurchania, R.K Pandey, J. Nano Sci. Nanotech, 13, pp.1812-1819 (2013).
24. S. Sen, P. Anand, M. Narjinary, S.K Md Mursalin, R. Manna, Ceramic Int, 42, pp.12581 (2016).
25. S. Peng, M. Ma, W. Yang, Z. Wang, J. Bi, Sens. Actuators B, 190, pp.627-633 (2014).